

An Investigation of a Potential Spin Liquid State in a Frustrated Triangular Lattice

M. B. Young

*Department of Mathematics and Statistics, Queen's University at Kingston,
Kingston, Ontario, K7L 3N6, Canada*

3my@qlink.queensu.ca

Abstract

We consider the Heisenberg model applied to a frustrated triangular lattice with nearest and next-nearest neighbour antiferromagnetic interactions. We find that the system may have spin liquid ground states for sufficiently strong next-nearest neighbour coupling. Before obtaining these results a brief review of the necessary background in quantum magnetism is presented and the theory of spin waves is developed.

Contents

1	Introduction	2
2	Quantum Magnetism	3
2.1	Ordering	3
2.2	Spin Liquids	5
2.3	Broken Symmetries	6
3	The Heisenberg Model	6
4	Spin Waves	8
4.1	Ferromagnetic Formalism	9
4.2	Remarks on the Antiferromagnetic Formalism	11
4.3	The Semi-Classical Interpretation	11
4.4	The Holstein-Primakoff Transformation	12
4.5	The Bogoliubov-Valatin Transformation	14
5	The Heisenberg Model on a Frustrated Square Lattice	15

6	Triangular Lattice	19
6.1	Three Boson Method	20
6.2	One Boson Method	22
6.3	Classical Results	25
7	Discussion	27

1 Introduction

The theory of magnetic systems is currently a major area of study in condensed matter physics with applications in high- T_c superconductivity and relations to fundamental questions in physics. The simplest and most studied model of magnetic systems is the Heisenberg model, represented by the spin Hamiltonian

$$H = \sum_{i \neq j} J_{ij} \hat{S}_i \cdot \hat{S}_j \quad (1)$$

where \hat{S}_i is a spin operator at a site i and J_{ij} are some constants. This model has been shown to be quite effective at describing the low temperature physics of many magnetic systems, most notably transition metal oxides [18]. The form of the Eq. (1) occurs because of the Coulomb repulsion between the localized electrons in the system.

Much of the work in quantum magnetism has centered around the low temperature behaviour of magnets where the quantum nature of the material is most important. The physics at low temperatures can be understood by analogy with the quantum harmonic oscillator. It is well known that the ground state energy of the harmonic oscillator is non-vanishing due to the zero-point quantum fluctuations which have energy $\frac{\hbar\omega}{2}$ for each degree of freedom. The same type of behaviour occurs at $T \approx 0$ in many magnetic systems and can be modeled by a system of harmonic oscillators. The quantum fluctuations in this case are called spin waves and have energy $\sum_k \frac{\hbar\omega(k)}{2}$, where k is the wavenumber of the spin wave. The calculation and study of $\omega(k)$ is the first step in using spin wave theory to understand the system at low temperatures.

In a large number of classical magnetic systems (i.e. we treat the spins in Eq. (1) as classical spin vectors) there does not exist a unique configuration of spins that minimize the energy. In fact, there are often an infinite number of degenerate ground states. The theory of spin waves was in part developed to answer the natural questions, Do the laws of quantum mechanics select a unique ground state? If quantum fluctuations do select a unique ground state, what symmetry does this state have? Is a given classical state stable under quantum fluctuations? The application of spin wave theory can be used to try and answer these and other questions as follows. We expand the Hamiltonian Eq. (1) in powers of $\frac{1}{S}$ around a classical ground state, the first order term in $\frac{1}{S}$ then corresponding to the first quantum contributions. Including only the constant and $\frac{1}{S}$ terms leads to linear spin wave

theory. We proceed to write the $\frac{1}{S}$ term in the form of a system of decoupled harmonic oscillators, in the process calculating the spin wave frequencies $\omega(k)$. Repeating this process for each of the degenerate ground states of the system and calculating the zero-point quantum energy in each case, we may then see that the quantum fluctuations choose a particular ground state, i.e. the ground state with the least energy added by quantum fluctuations. The selection of a quantum ground state by this method is called order from disorder. Of course, the calculation of $\omega(k)$ for a given configuration of spins is the non-trivial part of the problem.

One relatively new application of spin wave theory is to identify and study quantum spin liquids. Unlike the well-known ferromagnetic and antiferromagnetic configurations, a spin liquid state has no long-range magnetic order. In particular, the expectation value of the spin $\langle \hat{S} \rangle$ throughout the magnet must vanish. It is this fact that allows spin wave analysis to predict whether or not a given system displays characteristics of a spin liquid. We will see that the inclusion of the $\frac{1}{S}$ term in the expansion of the Hamiltonian induces a change in $\langle \hat{S} \rangle$. If the quantum fluctuations are large enough they may melt the classical ground state, i.e. reduce $\langle \hat{S} \rangle$ to zero, destroying the classical state to which the spin waves were applied. It was not until 1988 that an example of a spin liquid was first suggested when Chandra and Doucot [6] conjectured that the Heisenberg antiferromagnet on a square lattice with nearest and next-nearest neighbour interactions produced a spin liquid state. It was ten years later before the first candidate of a three dimensional quantum spin liquid was found in the pyrochlore antiferromagnet [5]. Spin liquids, having no long-range magnetic order, represent a class of magnetic systems unlike any others that have been previously studied. In order to better understand spin liquids and any associated novel orderings it is important to first have a library of examples of these systems.

The outline of this paper is as follows. We begin with a brief introduction to the basic concepts of quantum magnetism and then introduce the celebrated Heisenberg model for magnetic systems. We then formally introduce the notion of spin waves and develop the necessary tools to apply the theory. The application of spin wave theory is illustrated on the square lattice with nearest and next-nearest neighbour interactions, previously studied in [6]. We then consider the Heisenberg model on the frustrated triangular lattice and find that the classical 120° ground state is a potential spin liquid. The appendices contain additional technical material and an example of spin wave theory in three dimensions.

2 Quantum Magnetism

2.1 Ordering

In magnetic systems the most common type of magnetic order is long-range in nature and occurs below some critical temperature T_c . By long-range order we mean that the relative orientation

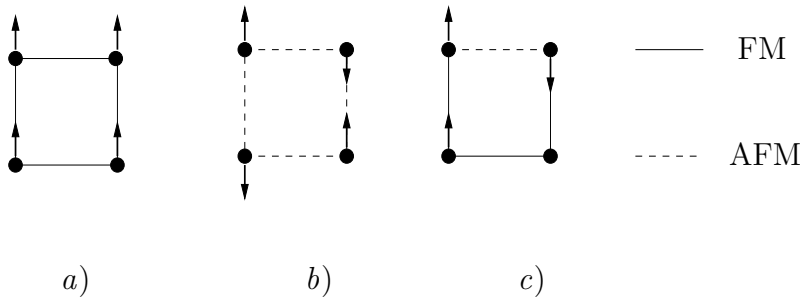


Figure 1: The square lattice with *a*) ferromagnetic interactions, *b*) antiferromagnetic interactions and *c*) mixed interactions between nearest neighbours. Ground states are shown in *a*) and *b*).

of spins is fixed, even at arbitrarily large distances. As a simple example of ordering we consider a square lattice with nearest neighbour ferromagnetic coupling, Figure 1*a*. The minimum energy for this lattice is obtained when all spins are collinear, in which case we say that the system has ferromagnetic order. Since we may orient the direction in which all spins point without changing the energy we see that the ground state is infinitely degenerate. However, this degeneracy is trivial in the sense that all such states are related by a rotation in spin space.

A second simple example of magnetic ordering is illustrated again by the square lattice, this time with nearest neighbour antiferromagnetic coupling, Figure 1*b*. The minimum energy state is achieved when neighbouring spins are anti-parallel; this is called the Néel state and is an example of antiferromagnetic order. These ground states share the same trivial degeneracy as the ferromagnetic states discussed above.

In the two cases just considered we have been able to find a unique (modulo rotational equivalence) ground state that possesses a distinct and characterizable type of long-range magnetic order. However it is easy to see that we cannot always expect to have such success. Indeed, consider a square lattice with both ferromagnetic and antiferromagnetic exchange, as in Figure 1*c*. Although the three spins illustrated minimize the interaction energies with their neighbours it is clear that the fourth spin cannot be chosen to do the same. In general, when all of the spins in a lattice cannot be chosen so as to satisfy all interactions the lattice is said to be frustrated. To be more precise, the frustration seen here is an example of frustration induced by disorder, i.e. because of the nature of the mixed interactions involved. Also of interest are geometrically frustrated lattices. One example of this is the triangular antiferromagnet with nearest neighbour interactions, Figure 2. It is clear from the figure that only two of the three interactions can be satisfied. We call this geometric frustration because the frustration is induced by the geometry of the lattice and not by mixed interactions.

A common feature of frustrated lattices is the presence of non-trivially degenerate ground states. That is, the states are not related by any particular symmetry. It is also often difficult to identify whether or not the ground states possess long-range order. Clearly, the order cannot always be

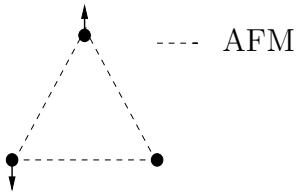


Figure 2: The triangular lattice with antiferromagnetic coupling. The third spin cannot be chosen so as to satisfy all interactions.

characterized as ferromagnetic or antiferromagnetic. Perhaps the most common order parameter is the so-called correlation function $\langle \hat{S}_i \cdot \hat{S}_j \rangle$ which measures the long-range magnetic order of a lattice with a fixed spin configuration as a function of the separation of the spins, $|r_i - r_j|$. We will see below that the correlation function helps to characterize spin liquids.

It is natural to ask what class of systems, if any, has no type of long-range magnetic order. In two dimensions it is known that the ground state of the Heisenberg antiferromagnet on the square lattice with nearest neighbour interactions has long range order for spins of at least 1, while there is considerable numerical evidence that the claim also holds for spin- $\frac{1}{2}$ lattices [18]. It was not until recently that examples of non-ordered systems began to appear.

2.2 Spin Liquids

It was predicted in 1983 that the antiferromagnetic spin-1 linear chain has a correlation function given by [18]

$$\langle \hat{S}_i \cdot \hat{S}_j \rangle \propto (-1)^{|i-j|} e^{-\frac{|r_i - r_j|}{\xi}} \quad (2)$$

where r_i is the position vector of the i^{th} spin and the quantity ξ is called the correlation length. If a magnetic system has a finite correlation length at $T = 0$ then we say that the system is a spin liquid. A system described by the correlation function Eq. (2) clearly cannot have ferromagnetic or antiferromagnetic ordering. In fact, Eq. (2) effectively says that the system has no long-range magnetic order at all, i.e. it is disordered. Thus, disordered systems may represent a type of novel ordering, one we have little knowledge of and would like to better understand.

One suggested example of a quantum spin liquid is the Heisenberg model on the spin- $\frac{1}{2}$ pyrochlore antiferromagnet. The pyrochlore lattice is a three dimensional arrangement of corner sharing tetrahedra and is an example of a geometrically frustrated system. In [5] it is predicted that ξ is finite for $T = 0$ and that the ground state degeneracy is lifted by quantum fluctuations; a collinear state in which the total spin on each tetrahedron vanishes is selected, consistent with the requirement that the ground state of a spin liquid be a singlet [18].

2.3 Broken Symmetries

From the form Heisenberg Hamiltonian Eq. (1) it is easy to see that it has rotational symmetry in spin space. That is, if R_θ is a rotation in spin space about some fixed axis by an angle θ , then the map $(\hat{S}_i, \hat{S}_j) \mapsto (R_\theta \hat{S}_i, R_\theta \hat{S}_j)$ leaves the Hamiltonian unchanged. However, as we have already seen, the eigenstates of Heisenberg Hamiltonian in general do not have such a symmetry. Indeed, even in the simple case of the ferromagnetic square lattice, the ground state is such that all spins point in some preferred direction and thus break the spin space symmetry of the Hamiltonian. A second symmetry of the Heisenberg Hamiltonian occurs in the case $J_{ij} \equiv J$ for some constant J , in which case the Hamiltonian is translation invariant. We see that the ferromagnetic square lattice ground state shares this symmetry. However, the ground state of the antiferromagnetic square lattice was seen above to induce a two sublattice structure, and hence breaks translational symmetry.

In general it is desirable to know the symmetry group of a ground state and how it relates to the symmetry group of its governing Hamiltonian. In particular, if the classical system has degenerate ground states we would like to understand the symmetry groups of the state chosen by quantum fluctuations to be the quantum ground state. What symmetries are broken in the quantum ground state and why? It is hoped that understanding what symmetries are passed from the Hamiltonian to its classical and quantum ground states will provide deeper insight into how these states are chosen and lead to a clearer understanding of the system itself.

3 The Heisenberg Model

The Heisenberg model has formed the basis for a large amount of work in the theory of magnetic systems since it first appeared in 1926. It is a model that attempts to describe the dynamics of spins on a lattice subject to the laws of quantum mechanics. In its most general form the model is described by the Heisenberg Hamiltonian

$$H = \sum_{i \neq j} J_{ij} \hat{S}_i \cdot \hat{S}_j.$$

Because the Heisenberg model will be the basis for the work done below we provide some motivation for its form. This work can be found in [10] and [21].

We begin by studying two different types of interactions that lead to Hamiltonians of the form $H \propto \hat{S}_1 \cdot \hat{S}_2$. Consider first a system with magnetically interacting dipoles, such as a molecule with two free electrons. Let $\vec{\mu}_i$, $i = 1, 2$, be dipole vectors and \vec{r} their separation vector. The Hamiltonian describing their interaction is

$$H = \frac{\vec{\mu}_1 \cdot \vec{\mu}_2}{r^3} - 3 \frac{(\vec{\mu}_1 \cdot \vec{r})(\vec{\mu}_2 \cdot \vec{r})}{r^5} - \frac{8\pi}{3} \vec{\mu}_1 \cdot \vec{\mu}_2 \delta(\vec{r}). \quad (3)$$

The term proportional to $\delta(\vec{r})$ arises due to terms of the form $\nabla \times \frac{\vec{\mu} \times \vec{r}}{r^3}$ in the expression for the magnetic field of the dipoles. If the two electrons are orbiting one another, the particle states are of the form $|l_i, m_i\rangle$, where l_i is the electron's angular momentum and m_i is magnetic quantum number. When viewed as a function of the direction of \vec{r} , $\langle l_1, m_2 | H | l_2, m_2 \rangle$ is a combination of spherical harmonics of degree two, so that $\langle l_1, m_2 | H | l_2, m_2 \rangle = 0$ unless $|l_1 - 2| \leq l_2 \leq l_1 + 2$. Since the wave functions behave like r^{l_i} near the origin, only the s states, i.e. $l_1 = l_2 = 0$, have non-zero wave functions at $r = 0$. Hence the $\delta(\vec{r})$ term contributes only to $\langle 0, m_2 | H | 0, m_2 \rangle$, while the first two terms in Eq. (3) can be shown to average to zero. Thus, for particles in a s state the interaction is proportional to $\vec{\mu}_1 \cdot \vec{\mu}_2$. Recall that $\vec{\mu}_i = g_i \frac{q_i}{2M_i c} \vec{S}_i$ where q_i is the charge of the particle, M_i its mass, c the speed of light and g_i the gyromagnetic ratio. Hence, the interaction is of the form $H = J \vec{S}_1 \cdot \vec{S}_2$ for some constant J , as desired. Observe that this spin-spin interaction is due to the direct magnetic interaction of the two dipoles.

As a second example of interactions of the form of the Heisenberg Hamiltonian consider a molecule with two electrons. Using the Born-Oppenheimer approximation and ignoring the spin of the nuclei we may describe each of the two electrons by their position \vec{r}_i and some component of their total spin \hat{S}_i . If $|\psi_a\rangle$ and $|\psi_b\rangle$ are two one-electron eigenstates of the molecule's Hamiltonian H' with eigenvalues E_a and E_b , respectively, then $|ab\rangle$ and $|ba\rangle$ are two-electron eigenstates with energy $E_a + E_b$, where we write $|ab\rangle = |\psi_a\rangle \otimes |\psi_b\rangle$, $|ba\rangle = |\psi_b\rangle \otimes |\psi_a\rangle$, with \otimes the tensor product between the two one-particle Hilbert spaces. We also include a mutual interaction potential V , such as the Coulomb potential, which is assumed to be spin independent and symmetric: $V(r_1, r_2) = V(r_2, r_1)$. Define the symmetric and antisymmetric states $|\psi_S\rangle = \frac{1}{\sqrt{2}}(|ab\rangle + |ba\rangle)$ and $|\psi_A\rangle = \frac{1}{\sqrt{2}}(|ab\rangle - |ba\rangle)$; both states are eigenvectors of the Hamiltonian with the interaction potential V , which we write as $H = H' + V$. We compute the energy of $|\psi_S\rangle$:

$$H|\psi_S\rangle = H'|\psi_S\rangle + V|\psi_S\rangle = (E_a + E_b)|\psi_S\rangle + V|\psi_S\rangle$$

so that

$$\langle \psi_S | H | \psi_S \rangle = (E_a + E_b) \langle \psi_S | \psi_S \rangle + \langle \psi_S | V | \psi_S \rangle = (E_a + E_b) + \langle ab | V | ab \rangle + \langle ab | V | ba \rangle.$$

If we define $I = \langle ab | V | ab \rangle$ and $J = -\langle ab | V | ba \rangle$ then $E_S = E_a + E_b + I - J$. A similar calculation shows that the energy of $|\psi_A\rangle$ is $E_A = E_a + E_b + I + J$.

To obtain the full electron wave function, we must tensor the spatial wave function $|\psi\rangle$ by a two electron spinor $\chi^{(s)}$ whose total spin is s . For spin- $\frac{1}{2}$ particles the symmetric states have total spin 1 while asymmetric states have vanishing total spin, so that by the Pauli exclusion principle we may write

$$|S\rangle = |\psi_S\rangle \otimes \chi^{(0)}, \quad |A\rangle = |\psi_A\rangle \otimes \chi^{(1)}.$$

If s is the total spin of the system and \hat{S} is the total spin operator of the system then the eigenvalues of $\hat{S} \cdot \hat{S}$ are $s(s+1) \in \{0, 2\}$. Hence, the energy E for both $|\psi_S\rangle$ and $|\psi_A\rangle$ can be compactly written

as

$$E = E_S + (E_A - E_S) \frac{s(s+1)}{2}.$$

From this we see that the interaction Hamiltonian is

$$H = E_S + \frac{(E_A - E_S)}{2} \hat{S} \cdot \hat{S}.$$

Recall that for spin- $\frac{1}{2}$ particles

$$\hat{S} \cdot \hat{S} = (\hat{S}_1 + \hat{S}_2) \cdot (\hat{S}_1 + \hat{S}_2) = \frac{3}{2} + 2\hat{S}_1 \cdot \hat{S}_2.$$

From this and the identity derived above for E_S and E_A in terms of E_a and E_b we find $H = E_a + E_b + I + \frac{1}{2}J + 2J\hat{S}_1 \cdot \hat{S}_2$. This result explicitly shows that the splitting in the energy levels is $\Delta H = 2J\hat{S}_1 \cdot \hat{S}_2$, which is again the form of the Heisenberg Hamiltonian. Note that even though V was assumed to be spin-independent, the interaction Hamiltonian is a spin-spin interaction. It is this Coulomb induced interaction that is of importance for the study of magnetic systems; this should be kept in mind throughout the paper.

Although this second derivation of Eq. (1) was quantum mechanical in nature, we could also allow \vec{S}_i be a classical spin vector, in which case the resulting Hamiltonian Eq. (1) describes the classical Heisenberg model. It is important to note that the classical Heisenberg model corresponds to the $S \rightarrow \infty$ quantum Heisenberg model. The defining difference between a classical spin vector and a quantum spin operator is that the projection of a classical spin vector on some axis may take any value between $-S$ and S , whereas the corresponding quantum spin operator may take only the $2S + 1$ values $-S, -S + 1, \dots, S - 1, S$. As $S \rightarrow \infty$ the quantum operators can then take arbitrarily many values. If we rescale the quantum operators by $\frac{1}{S}$ we see that the spectrum of the projection becomes dense in $[-1, 1]$, which is just the spectrum of the projected classical spin vectors (also rescaled, of course), so that the $S \rightarrow \infty$ limit of the quantum Heisenberg model is indeed the classical Heisenberg model. That this is so is an essential component of spin wave theory, as we will see below.

Remark 3.1. *Had we considered systems with higher spin values (i.e. $S = 1, \frac{3}{2}, \dots$), we would have arrived at $\Delta H \propto$ (polynomial in $\hat{S}_1 \cdot \hat{S}_2$).*

4 Spin Waves

Given a magnetic system described by the Heisenberg model we would like to be able to determine the ground state spin configuration and its energy, the magnetic susceptibility and so forth. Although the Heisenberg model is the simplest available to describe magnetic systems, it is impossible in nearly all interesting cases to calculate exact quantities, a situation reminiscent of quantum mechanics, and as such it is necessary to develop approximate techniques. One approximate method

is given by the theory of spin waves, which amounts to an expansion in $\frac{1}{S}$ of the the Heisenberg Hamiltonian. As noted above the $S \rightarrow \infty$ limit of the Heisenberg Hamiltonian describes the classical model. Consider then a magnetic system with classical ground state $|0\rangle_{cl}$ and energy E_{cl} . Expanding Eq. (1) to first order in $\frac{1}{S}$ we have a Hamiltonian of the form $H_{cl} + \frac{1}{S}H'$ where H' describes the first order quantum effects and $H_{cl}|0\rangle_{cl} = E_{cl}|0\rangle_{cl}$. Using spin wave theory we attempt to write the expanded Hamiltonian in the form of a system of harmonic oscillators, $H_{cl} + \sum_k \hbar\omega(k) \left(c_k^\dagger c_k + \frac{1}{2} \right)$ where c_k and c_k^\dagger are Bose annihilation and creation operators, respectively.¹ See Appendix A for a review of the quantum harmonic oscillator. We interpret the action of c_k^\dagger on $|0\rangle_{cl}$ as the creation of a spin wave of wave number k . When the Hamiltonian is written in this form the ground state energy for the quantum system is

$$E_{GS} = E_{cl} + \frac{1}{2} \sum_k \hbar\omega(k) + O\left(\frac{1}{S^2}\right).$$

We say that we have *dressed* the classical ground state $|0\rangle_{cl}$ with spin waves.

The above formalism describes how to approximate the energy of a classical ground state when viewed as a configuration of spins in the quantum model. Let us consider the case in which the ground state of the classical Hamiltonian is degenerate. Write the degenerate states as $|\psi_\alpha\rangle$, $\alpha \in \mathcal{A}$ for some indexing set \mathcal{A} . We perform spin wave analysis on each $|\psi_\alpha\rangle$ to obtain the corresponding approximate quantum energies, $E_\alpha = E_{cl} + \frac{1}{2} \sum_k \hbar\omega_\alpha(k)$, $\alpha \in \mathcal{A}$. We may then compare the sums $\frac{1}{2} \sum_k \hbar\omega_\alpha(k)$ to see whether the quantum ground state fluctuations lift the degeneracy of the classical system. That is, does there exist a unique $\alpha_0 \in \mathcal{A}$ such that

$$\frac{1}{2} \sum_k \hbar\omega_{\alpha_0}(k) < \frac{1}{2} \sum_k \hbar\omega_\alpha(k) \quad \forall \alpha \in \mathcal{A} \setminus \{\alpha_0\}?$$

If such a α_0 exists, then we say that the quantum fluctuations lift the degeneracy of the system, choosing the state $|\psi_{\alpha_0}\rangle$ as the quantum ground state.

We introduce spin waves below in the context of ferromagnetic systems. After doing so, we briefly describe the theory for antiferromagnetic lattices and finally present a semi-classical interpretation which justifies the physical intuition developed in the next two sections.

4.1 Ferromagnetic Formalism

To best understand spin waves we will first consider a one dimensional $S = \frac{1}{2}$ ferromagnet with the circular topology. The work in this subsection follows [10]. The spin physics for $S = \frac{1}{2}$ is best understood using the Pauli spin matrices σ^i , $i \in \{x, y, z\}$, with which the spin operator is $\hat{S} = \frac{1}{2}\sigma$, where $\sigma = \sigma^x \hat{x} + \sigma^y \hat{y} + \sigma^z \hat{z}$. Note that we have set $\hbar = 1$. Denote the spin on the i^{th} vertex

¹There may exist an arbitrary number of quantum fluctuations (spin waves) throughout the lattice at a given time, so that spin waves obey bosonic spin statistics.

by $\hat{S}_i = \frac{1}{2}\sigma_i$ and the distance between neighbouring spins by a . Including only nearest neighbour coupling, Eq. (1) gives

$$H = -J \sum_{n=1}^N \sigma_n \cdot \sigma_{n+1} \quad (4)$$

with J suitably rescaled. That the interactions on the lattice are ferromagnetic is reflected in the condition $J > 0$. With this, having neighbouring spins parallel minimizes the energy of the system, as to be expected for ferromagnets. Note that $\sigma_{N+1} = \sigma_1$, as dictated by the topology of the lattice. It is natural to ask why we have taken the topology of the lattice to be circular rather than linear. The main reason is that the circular topology simplifies the following calculations. From a physical point of view, in the thermodynamic limit $N \rightarrow \infty$ the topology differences of the circle and line become negligible, so that the topology of the finite lattice is of little importance.

Fix a direction in spin space; call this direction up. Denote by $|\alpha\rangle$ and $|\beta\rangle$ spin up and down states, respectively. Note that the set $\{|\alpha\alpha\rangle, |\alpha\beta\rangle, |\beta\alpha\rangle, |\beta\beta\rangle\}$ forms an orthonormal basis for the two-particle spin Hilbert space. Introduce the spin exchange operator $p^{1,2} = \frac{1}{2}(1 + \sigma_1 \cdot \sigma_2)$. Its actions on the basis states are easily seen to be

$$p^{1,2}|\alpha\alpha\rangle = |\alpha\alpha\rangle, \quad p^{1,2}|\beta\beta\rangle = |\beta\beta\rangle, \quad p^{1,2}|\alpha\beta\rangle = |\beta\alpha\rangle, \quad p^{1,2}|\beta\alpha\rangle = |\alpha\beta\rangle.$$

From the definition of $p^{1,2}$ we write Eq. (4) as

$$H = -J \sum_{n=1}^N (2p^{n,n+1} - 1) = NJ - 2J \sum_{n=1}^N p^{n,n+1}. \quad (5)$$

As stated above we expect that the lowest energy state will be that with the most symmetry. In particular the states $|\alpha \cdots \alpha\rangle$ and $|\beta \cdots \beta\rangle$ should have the lowest energy. That this is so can be seen from the action of the spin exchange operator on the basis states; the completely symmetric states are eigenvectors of this operator with maximal eigenvalue and hence minimize the energy. That these states are exact eigenvalues of the Hamiltonian is what makes the ferromagnetic case so easy to solve. A calculation shows that $E = \langle \alpha \cdots \alpha | H | \alpha \cdots \alpha \rangle = -NJ$. For simplicity, we make the transformation $H \mapsto H + NJ$ so that we have $E = \langle \alpha \cdots \alpha | H | \alpha \cdots \alpha \rangle = 0$. Similarly, the energy of the state $|\beta \cdots \beta\rangle$ vanishes. In fact, any state in which the projection of all spins onto a fixed direction in spin space is maximal will be an eigenvector of H with vanishing eigenvalue. This is a reflection of the rotational symmetry of H in spin space.

To find the first excited state one might suggest the state with one spin down and the rest up, $|\alpha \cdots \alpha \beta \alpha \cdots \alpha\rangle$, but this is easily seen to not be an eigenvector. However such vectors do form a basis for the Hilbert space of the system. Define the vectors

$$|\varphi_i\rangle = |\alpha \cdots \alpha \beta \alpha \cdots \alpha\rangle, \quad \forall i \in \{1, \dots, N\}$$

where β is in the i^{th} position. A general state $|\varphi\rangle$ in the Hilbert space may be expanded in this basis as $|\varphi\rangle = \sum_{n=1}^N c_n |\varphi_n\rangle$, $c_n \in \mathbb{C}$. Observe that $p^{n,n+1}|\varphi_n\rangle = |\varphi_{n+1}\rangle$ and $p^{n-1,n}|\varphi_n\rangle = |\varphi_{n-1}\rangle$, $\forall n \in \{1, \dots, N\}$. Using this, we compute

$$H|\varphi\rangle = -2J \sum_{n=1}^N c_n (-2|\varphi_n\rangle + |\varphi_{n+1}\rangle + |\varphi_{n-1}\rangle).$$

If $|\varphi\rangle$ is an eigenvector of H , then $(H - E)|\varphi\rangle = 0$. Requiring this and using the orthonormality of $\{|\varphi_n\rangle\}_n$ we find $Ec_n = -2J(-2c_n + c_{n+1} + c_{n-1})$. Using Bloch's Theorem (see Appendix B) we set $c_n = e^{i\zeta n}$ for some $\zeta \in \mathbb{R}$. This implies $E = -2J(-2 + e^{i\zeta} + e^{-i\zeta})$, or equivalently, $E = 4J(1 - \cos \zeta)$. Because of the boundary conditions (i.e. the circular topology of the lattice) we require $1 = e^{iN\zeta}$, which implies

$$\zeta = \frac{2\pi l}{N}, \quad l \in \mathbb{Z} \cap \left[-\frac{N}{2}, \frac{N}{2}\right].$$

Defining the wave number $k = \frac{\zeta}{a}$ we can write

$$E = 4J(1 - \cos ka). \quad (6)$$

For k small, this gives the long wavelength approximation $E \approx 2Ja^2k^2$. Note that if $\zeta = 0$, or equivalently $k = 0$, then $E = 0$ by Eq. (6). That is, $\sum_{n=1}^N |\varphi_n\rangle$ is a ground state of H . That this is so can also be seen by noting that such a state is completely symmetric. If $\zeta \neq 0$ then the spins at each vertex are out of phase, leading to a propagating disturbance of spins throughout the lattice, i.e. a spin wave. The semi-classical interpretation described below will justify this intuitive picture.

4.2 Remarks on the Antiferromagnetic Formalism

The antiferromagnetic analysis is significantly more complicated than the ferromagnetic case studied above. To study the antiferromagnetic case we set $J_{ij} \equiv J > 0$ in Eq. (1) and consider only nearest neighbour interactions, so that neighbouring spins tend to be anti-parallel. The classical ground state, as noted above, is the Néel state in which all neighbouring spins anti-parallel. However, writing the Hamiltonian in the form Eq. (5) we see that the Néel state is not an exact eigenvector of the quantum system. This fact prevents the antiferromagnetic case from being solved using the same method as above. We omit the details here as they will not be necessary for understanding what is to follow. We do however note that one difference in the antiferromagnetic case is that in the long wavelength approximation we find $E \propto k$. For details see [2], [15].

4.3 The Semi-Classical Interpretation

From the form of the eigenvector $|\varphi\rangle$ found in the Section 4.1 we may view the effect of spin waves on the lattice as tipping the spin vectors away from the up direction in a way such that neighbouring

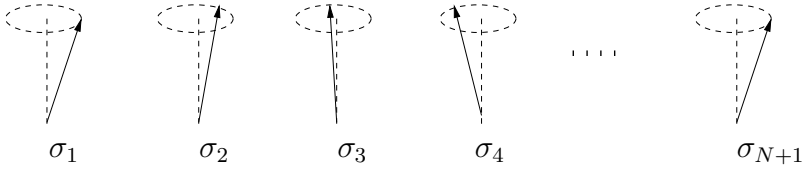


Figure 3: The semi-classical interpretation of spin waves in a linear ferromagnetic chain with N vertices.

spins are out of phase. This is illustrated in Figure 3. We would like to check that indeed this intuition accurately reflects the formalism we have developed. We again follow [10].

We begin with the ferromagnetic Hamiltonian $H = -J \sum_{n=1}^N (\sigma_n \cdot \sigma_{n+1} - 1)$. We wish to find a classical equation of motion to describe the spin vectors σ_n . To do this, we will use the Heisenberg equation of motion $\dot{\sigma}_n = i[H, \sigma_n]$, which implies $\dot{\sigma}_n = iJ[\sigma_n \cdot \sigma_{n+1}, \sigma_n]$. A computation shows that $[\sigma_n \cdot \sigma_{n+1}, \sigma_n] = 2i\sigma_n \times \sigma_{n+1}$ so that we arrive at $\dot{\sigma}_n = 2J\sigma_n \times (\sigma_{n+1} - \sigma_{n-1})$. These equations are much easier to solve in their linearization. To do this, say $\sigma_{n,z} \approx 1$ for all n , i.e. we assume the spins do not deviate greatly from their classical direction. The above equations become

$$\dot{\sigma}_n^x \approx 2J(2\sigma_n^y - \sigma_{n+1}^y - \sigma_{n-1}^y), \quad \dot{\sigma}_n^y \approx -2J(2\sigma_n^x - \sigma_{n+1}^x - \sigma_{n-1}^x).$$

Recall that in the linear ferromagnet the low energy excitations of the lattice were found to be spin waves. This motivates the ansatz

$$\sigma_n^x = Ce^{inak} \sin \omega t, \quad \sigma_n^y = Ce^{inak} \cos \omega t$$

for some constants C and ω . These two solutions describe the spin dynamics pictured in Figure 3. Substitution of this in the linearized equation for σ_n^x , say, implies

$$\omega = 4J(1 - \cos ka).$$

If we set $E = \omega$ then we recover Eq. (6). Hence we see that the semi-classical interpretation agrees with the strict quantum understanding of spin waves. It will be useful to keep this interpretation in mind when thinking about spin waves in what is to follow.

4.4 The Holstein-Primakoff Transformation

The next step towards a formal theory of spin waves is an appropriate algebraic representation of the spin operators. We follow here the construction given in [16]. For an alternative approach see [17].

Consider a lattice with spin operators \hat{S}_r^z on each lattice site r . Define the spin deviation operator $\hat{n}_r = S - \hat{S}_r^z$ which measures the amount the spin at r deviates from the maximal z component of the spin. Denote by $|n_r\rangle$ an eigenvector of \hat{n}_r with eigenvalue n_r . Note that $n_r \in \{0, \dots, 2S\}$. The

Hilbert space of is then spanned by states of the form $\bigotimes_r |n_r\rangle$. In this basis \hat{S}_r^z is diagonal since $\hat{S}_r^z |n_r\rangle = (S - n_r) |n_r\rangle$. However the spin raising and lowering operators are not:

$$\hat{S}_r^+ |n_r\rangle = \sqrt{2S \left(1 - \frac{n_r - 1}{2S}\right)} n_r |n_r - 1\rangle, \quad \hat{S}_r^- |n_r\rangle = \sqrt{2S (n_r + 1) \left(1 - \frac{n_r}{2S}\right)} n_r |n_r + 1\rangle.$$

Define the operators \hat{a}_r and \hat{a}_r^\dagger by $\hat{a}_r |n_r\rangle = \sqrt{n_r} |n_r - 1\rangle$ and $\hat{a}_r^\dagger |n_r\rangle = \sqrt{n_r + 1} |n_r + 1\rangle$. Then if $f(x) = \sqrt{1 - \frac{x}{2S}}$, we claim

$$\hat{S}_r^+ = \sqrt{2S} f(\hat{n}_r) \hat{a}_r, \quad \hat{S}_r^- = \sqrt{2S} \hat{a}_r^\dagger f(\hat{n}_r),$$

and

$$\hat{n}_r = \hat{a}_r^\dagger \hat{a}_r. \quad (7)$$

It is sufficient to check that the left and right hand sides of the above equations agree on the basis states $|n_r\rangle$. For instance,

$$\sqrt{2S} f(\hat{n}_r) \hat{a}_r |n_r\rangle = \sqrt{2S n_r} f(\hat{n}_r) |n_r - 1\rangle = \sqrt{2S n_r} \sqrt{1 - \frac{n_r - 1}{2S}} |n_r - 1\rangle = \hat{S}_r^+ |n_r\rangle$$

as claimed. Using the identities $\hat{S}_r^x = \frac{1}{2} (\hat{S}_r^+ + \hat{S}_r^-)$ and $\hat{S}_r^y = \frac{1}{2i} (\hat{S}_r^+ - \hat{S}_r^-)$ we also have expressions for \hat{S}_r^x and \hat{S}_r^y . For example, $\hat{S}_r^x = \sqrt{\frac{S}{2}} (f(\hat{n}_r) \hat{a}_r + \hat{a}_r^\dagger f(\hat{n}_r))$ which after Taylor expanding becomes

$$\hat{S}_r^x = \sqrt{\frac{S}{2}} (\hat{a}_r + \hat{a}_r^\dagger) + O\left(\frac{1}{S}\right). \quad (8)$$

Following the same procedure with the y component of the the spin we find

$$\hat{S}_r^y = -i \sqrt{\frac{S}{2}} (\hat{a}_r - \hat{a}_r^\dagger) + O\left(\frac{1}{S}\right). \quad (9)$$

The approximate forms of the spin operators Eqs. (7), (8) and (9) make up the so-called Holstein-Primakoff transformation. This transformation will be used extensively in the results that follow.

Remark 4.1. *The form of the Holstein-Primakoff transformation derived above is obtained by expanding the spin operators to first order in $\frac{1}{S}$. One can easily take more terms in the series expansion of $f(\hat{n}_r)$ to obtain higher order expansions of the spin operators. We will not do so here, as we are interested in linear spin wave theory; the introduction of non-linear terms into the Holstein-Primakoff transformation creates substantial challenges in the application of spin wave theory.*

4.5 The Bogoliubov-Valatin Transformation

If a_k is a Bose operator,² consider a transformation of the form

$$a_k = \mu_k c_k + \eta_k c_{-k}^\dagger \quad (10)$$

where $\mu_k, \eta_k \in \mathbb{C}$ with $\mu_k = \mu_{-k}$ and $\eta_k = \eta_{-k}$ and c_k are some new operators. Such a transformation is called a Bogoliubov-Valatin transformation [20]. Observe that, using $[a_k, a_k^\dagger] = 1$,

$$[c_k, c_k^\dagger] = [\mu_k a_k + \eta_k a_{-k}^\dagger, \mu_k^* a_k^\dagger + \eta_k^* a_{-k}] = |\mu_k|^2 - |\eta_k|^2.$$

If the new operators c_k are to represent Bosons we require $[c_k, c_k^\dagger] = 1$, which holds if and only if the hyperbolic normalization condition holds:

$$|\mu_k|^2 - |\eta_k|^2 = 1. \quad (11)$$

In particular, putting $\mu_k = \cosh \theta_k$ and $\eta_k = \sinh \theta_k$ is sufficient to satisfy Eq. (11). In what follows below, we assume $\mu_k \in \mathbb{R}$ and $\eta_k \in \mathbb{R}$.

We illustrate the application of the Bogoliubov-Valatin transformation with an example that will be useful below. Consider a Hamiltonian of the form

$$H = \sum_k \left[A_k a_k^\dagger a_k - \frac{B_k}{2} (a_k a_{-k} + a_k^\dagger a_{-k}^\dagger) \right]. \quad (12)$$

Inserting the transformation Eq. (10) and using $\sum_k c_{-k}^\dagger c_{-k} = \sum_k c_k^\dagger c_k$ this becomes

$$H = \sum_k \left\{ [A_k (\mu_k^2 + \eta_k^2) - 2B_k \mu_k \eta_k] c_k^\dagger c_k + \left[A_k \mu_k \eta_k - \frac{B_k}{2} (\mu_k^2 + \eta_k^2) \right] (c_k^\dagger c_{-k}^\dagger + c_k c_{-k}) + A_k \eta_k^2 - B_k \mu_k \eta_k \right\}.$$

Since the coefficients of $c_k^\dagger c_{-k}^\dagger$ and $c_k c_{-k}$ are identical, imposing $A_k \mu_k \eta_k - \frac{B_k}{2} (\mu_k^2 + \eta_k^2) = 0$ ensures that the non-diagonal terms vanish and hence diagonalizes the Hamiltonian. It is convenient to rewrite this constraint as

$$\frac{2\mu_k \eta_k}{\mu_k^2 + \eta_k^2} = \frac{B_k}{A_k} \equiv \gamma_k. \quad (13)$$

We now turn our attention to the constant term. Using Eq. (11), we write $\eta_k^2 = \frac{1}{2} (\mu_k^2 + \eta_k^2 - 1)$, so that the constant terms become $\frac{1}{2} A_k (\mu_k^2 + \eta_k^2) (1 - \gamma_k^2) - \frac{1}{2} A_k$. Using this, the diagonalized Hamiltonian reads

$$H = H_0 + \sum_k \omega(k) \left(c_k^\dagger c_k + \frac{1}{2} \right) \quad (14)$$

²For the rest of the text we omit the operator hat $\hat{}$ on Bose operators so as to reduce clutter in already complicated equations.

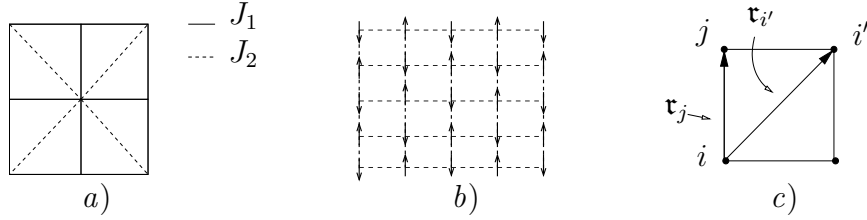


Figure 4: The figure shows *a*) the nearest and next-nearest neighbour couplings in the square lattice, *b*) the Néel ground state and *c*) the displacement vectors $\mathbf{r}_{i'}$ and \mathbf{r}_j .

where $H_0 = -\frac{1}{2} \sum_k A_k$ and $\omega(k) = A_k (\mu_k^2 + \eta_k^2) (1 - \gamma_k^2)$. We have thus transformed the Hamiltonian into the form of decoupled harmonic oscillators. Hence starting from a Hamiltonian of the form Eq. (12) we can use that Bogoliubov-Valatin transformation to put H in a form that makes the zero-point quantum fluctuations apparent.

5 The Heisenberg Model on a Frustrated Square Lattice

As a first example of the application of spin wave theory we consider the previously studied [6] Heisenberg model on a square lattice with nearest (J_1) and next-nearest (J_2) neighbour antiferromagnetic interactions (see Figure 4*a*). The addition of next-nearest neighbour interactions adds frustration to the system since the ground state of the $J_2 = 0$ case is the Néel state (Figure 4*b*); this configuration satisfies all nearest neighbour interactions and no next-nearest neighbour interactions, so that as $\lambda \equiv \frac{J_2}{J_1}$ grows the frustration increases. We will use the techniques developed above to find the first quantum corrections to the ground state magnetization $\langle \hat{S} \rangle$ as a function of λ .

We begin the calculation by dividing the lattice into two sublattices, labeled by A and B . On the A sublattice all spins point up, while on the B sublattice all spins point down (Figure 4*b*). Hence, the nearest neighbours to a point in A all lie in B , while the next-nearest neighbours to a point in A lie only in A . We carry out the calculation assuming each sublattice has only N vertices and take the $N \rightarrow \infty$ limit at the end. We label points on the A sublattice by i and those on the B sublattice by j . The distance between nearest neighbours is a . We may then write the Hamiltonian as

$$H = J_1 \sum_{\langle i,j \rangle} \hat{S}_i \cdot \hat{S}_j + J_2 \sum_{\langle i,i' \rangle} \hat{S}_i \cdot \hat{S}_{i'} + J_2 \sum_{\langle j,j' \rangle} \hat{S}_j \cdot \hat{S}_{j'}.$$

The notations $\sum_{\langle i,j \rangle}$ and $\sum_{\langle i,i' \rangle}$ indicate a sum over all nearest neighbours i and j and a sum over all next-nearest neighbours i and i' , respectively. Using the Holstein-Primakoff transformation Eqs. (7), (8) and (9) for two different types of Bose operators gives

$$\hat{S}_i \cdot \hat{S}_j = -\hat{S}_i^x \hat{S}_j^x + \hat{S}_i^y \hat{S}_j^y - \hat{S}_i^z \hat{S}_j^z = -S^2 + S \left(a_i^\dagger a_i + b_j^\dagger b_j \right) - S \left(a_i b_j + a_i^\dagger b_j^\dagger \right)$$

and

$$\hat{S}_i \cdot \hat{S}_{i'} = S^2 - S \left(a_i^\dagger a_i + a_{i'}^\dagger a_{i'} \right) - S \left(a_i a_{i'}^\dagger + a_i^\dagger a_{i'} \right),$$

with an analogous expression holding for $\hat{S}_j \cdot \hat{S}_{j'}$. We have written a_i for a Bose operator on A and b_j for a Bose operator on B . The Hamiltonian can then be written as

$$\begin{aligned}
H = & 4NS^2 (-J_1 + J_2) NS^2 + J_1 S \sum_{\langle i,j \rangle} (a_i^\dagger a_i + b_j^\dagger b_j) - J_1 S \sum_{\langle i,j \rangle} (a_i b_j + a_i^\dagger b_j^\dagger) \\
& - J_2 S \sum_{\langle i,i' \rangle} (a_i^\dagger a_i + a_{i'}^\dagger a_{i'}) + J_2 S \sum_{\langle i,i' \rangle} (a_i^\dagger a_{i'} + a_i a_{i'}^\dagger) \\
& - J_2 S \sum_{\langle j,j' \rangle} (b_j^\dagger b_j + b_{j'}^\dagger b_{j'}) + J_2 S \sum_{\langle j,j' \rangle} (b_j^\dagger b_{j'} + b_j b_{j'}^\dagger)
\end{aligned} \tag{15}$$

where we have used the fact that to each vertex there are four nearest neighbours and four next-nearest neighbours. Because Eq. (15) has two types of Bose operators we introduce two types of Fourier transformed operators

$$a_k = \frac{1}{\sqrt{N}} \sum_{i \in A} e^{ik \cdot r_i} a_i, \quad b_k = \frac{1}{\sqrt{N}} \sum_{j \in B} e^{ik \cdot r_j} b_j.$$

The following proposition will be useful in what follows.³

Proposition 5.1. *Let $k_n = \frac{2\pi n}{N}$, $n = 1, \dots, N$. Then,*

$$\sum_{l=1}^N e^{i(k_m - k_n)l} = N \delta_{m,n}$$

where $\delta_{m,n}$ is the Kronecker delta.

Proof. We write

$$\frac{1}{N} \sum_{l=1}^N e^{-i(k_m - k_n)l} = \frac{1}{N} \sum_{l=1}^N e^{-i \frac{2\pi i}{N} (m-n)l}.$$

Recall that for any $z \in \mathbb{C} \setminus \{1\}$, $n \neq 1$, we have $\sum_{l=1}^N z^l = \frac{z^{N+1} - 1}{z - 1}$. If $m \neq n$, setting $z = e^{-i \frac{2\pi i}{N} (m-n)}$ in the above results gives $\sum_{l=1}^N e^{-i(k_m - k_n)l} = 0$, while if $m = n$, we have $e^{-i(k_m - k_n)l} = 1$, so that $\sum_{l=1}^N e^{-i(k_m - k_n)l} = N$ which proves the desired result. \square

It remains to Fourier transform the non-diagonal components of Eq. (15). We compute

$$\sum_{\langle i,i' \rangle} a_i^\dagger a_{i'} = \frac{1}{N} \sum_{\langle i,i' \rangle} \sum_{k,k' \in \mathcal{B}} e^{i(k \cdot r_i - k' \cdot r_{i'})} a_k^\dagger a_{k'}.$$

The set \mathcal{B} is the first Brillouin zone whose construction is detailed in Appendix C. The actual form of \mathcal{B} is not important until we take the thermodynamic limit below. Since the sum is over next nearest neighbours, for a fixed i we can unambiguously label each next-nearest neighbour by a vector

³Proposition 5.1 is directly applicable to the one dimensional linear chain. However its application to lattices of higher dimension, such as the square lattice, is immediate.

$\mathbf{r}_{i'}$ that is based at the vertex i and points to the vertex i' in question (Figure 4c). The geometry of the lattice implies that $\mathbf{r}_{i'} = a(u\hat{x} + u'\hat{z})$ with $u, u' \in \{1, -1\}$ taking all four permutations. This allows the sum to be written as

$$\sum_{\langle i, i' \rangle} a_i^\dagger a_{i'} = \sum_{k \in \mathcal{B}} \left(\sum_{i'} e^{ik \cdot \mathbf{r}_{i'}} \right) a_k^\dagger a_k$$

where we have used Proposition 5.1 to evaluate the sum over i and k' . We define $\beta_k = \frac{1}{4} \sum_{i'} e^{ik \cdot \mathbf{r}_{i'}}$. Using the form of $\mathbf{r}_{i'}$ given above the explicit form of β_k is seen to be $\beta_k = \cos k_x a \cos k_y a$. Analogous computations show

$$\sum_{\langle i, i' \rangle} a_i a_{i'} = 4 \sum_{k \in \mathcal{B}} \beta_k a_k a_{-k}, \quad \sum_{\langle i, i' \rangle} a_i^\dagger a_{i'}^\dagger = 4 \sum_{k \in \mathcal{B}} \beta_k a_k^\dagger a_{-k}^\dagger, \quad \sum_{\langle i, j \rangle} a_i b_j = 4 \sum_{k \in \mathcal{B}} \alpha_k a_k b_{-k}$$

and so on, where $\alpha_k = \frac{1}{4} \sum_j e^{ik \cdot \mathbf{r}_j}$ with \mathbf{r}_j the vector that is based at vertex i and points to the nearest neighbour vertex j (Figure 4c). Explicitly, $\alpha_k = \frac{1}{2} (\cos k_x a + \cos k_y a)$. Putting this all together, the Fourier transformed Hamiltonian reads

$$\begin{aligned} H = 4NS^2 (-J_1 + J_2) + 8J_2S \sum_{k \in \mathcal{B}} \beta_k + 4S \sum_{k \in \mathcal{B}} [J_1 - J_2(1 - \beta_k)] \left(a_k^\dagger a_k + b_k^\dagger b_k \right) \\ - 4J_1S \sum_{k \in \mathcal{B}} \alpha_k \left(a_k b_{-k} + a_k^\dagger b_{-k}^\dagger \right). \end{aligned} \quad (16)$$

We now introduce the Bogoliubov-Valatin transformation

$$a_k = \cosh \theta_k c_k + \sinh \theta_k d_k^\dagger, \quad b_k = \cosh \theta_k d_k + \sinh \theta_k c_k^\dagger$$

to diagonalize the Hamiltonian. This is a straightforward generalization to two Bose operators of the single Bose operator Bogoliubov-Valatin transformation Eq. (10). Substituting this in Eq. (16), the coefficients of $c_k d_k$ and $c_k^\dagger d_k^\dagger$ are both found to be

$$2 [J_1 - J_2 (1 - \beta_k)] \cosh \theta_k \sinh \theta_k - J_1 \alpha_k (\sinh^2 \theta_k + \cosh^2 \theta_k).$$

Requiring both terms vanish imposes a constraint on the function θ_k ,

$$\tanh 2\theta_k = \frac{\alpha_k}{1 - \lambda(1 - \beta_k)} \equiv \gamma_k. \quad (17)$$

Rewriting Eq. (16) in terms of the new operators c and d we find

$$H = H_\lambda^0 + \sum_{k \in \mathcal{B}} \omega_\lambda(k) \left(c_k^\dagger c_k + d_k^\dagger d_k + 1 \right) \quad (18)$$

where

$$\omega_\lambda(k) = J_1 S [1 - \lambda(1 - \beta_k)] \sqrt{1 - \gamma_k^2}. \quad (19)$$

and $H_\lambda^0 = 4J_1NS^2(-1 + \lambda) + 8J_2S \sum_{k \in \mathcal{B}} \beta_k$, which is again of the form of a system of decoupled harmonic oscillators.

We can use the above formalism to calculate the reduction of the moment on a single sublattice due to quantum fluctuations. Note that $\langle \hat{S} \rangle_A = \langle S - \sum_{i=1}^N a_i^\dagger a_i \rangle = \langle S - \sum_{k \in \mathcal{B}} a_k^\dagger a_k \rangle$, with the same expression holding for the B sublattice. Inserting the Bogoliubov-Valatin transformation we find $\langle \hat{S} \rangle = S - \sum_{k \in \mathcal{B}} \sinh^2 \theta_k$. Using the identity $\tanh 2x = \frac{2 \sinh x \sqrt{1 + \sinh^2 x}}{1 + 2 \sinh^2 x}$ we find an equation in terms of γ_k and $\sinh \theta_k$:

$$(1 + 2 \sinh^2 \theta_k)^2 \gamma_k^2 = 4 \sinh^2 \theta_k (1 + \sinh^2 \theta_k).$$

Solving we find $\sinh^2 \theta_k = \frac{1}{2} \left(\frac{1}{\sqrt{1 - \gamma_k^2}} - 1 \right)$ so that

$$\frac{\langle \hat{S} \rangle}{S} = 1 - \frac{1}{2S} \sum_{k \in \mathcal{B}} \left(\frac{1}{\sqrt{1 - \gamma_k^2}} - 1 \right). \quad (20)$$

Using this result, in the thermodynamic limit ($N \rightarrow \infty$) the reduction of the moment on each sublattice is

$$\frac{\langle \hat{S} \rangle}{S} = 1 + \frac{1}{2S} - \frac{1}{8\pi^2 S} \iint_{\mathcal{B}_\infty} d^2k \frac{1 - \lambda(1 - \beta_k)}{\sqrt{[1 - \lambda(1 - \beta_k)]^2 - \alpha_k^2}} \quad (21)$$

where $\mathcal{B}_\infty = [-\pi, \pi] \times [-\pi, \pi]$ is the first Brillouin zone for $N \rightarrow \infty$. This result agrees with that derived in [6].⁴ We have also transformed the sum into an integral because \mathcal{B} is now a continuous set:

$$\sum_{k \in \mathcal{B}} \mapsto \frac{1}{(2\pi)^2} \iint_{\mathcal{B}_\infty} d^2k \quad \text{as } N \rightarrow \infty.$$

We would like to determine for a given value of spin S whether or not there exists a λ such that the reduction of the moment is reduced to zero. Setting $I_\lambda = \frac{1}{8\pi^2} \iint_{\mathcal{B}_\infty} d^2k \frac{1 - \lambda(1 - \beta_k)}{\sqrt{[1 - \lambda(1 - \beta_k)]^2 - \alpha_k^2}}$, we see that the curve in $\frac{1}{S} - \lambda$ space on which the reduction vanishes is given by the equation

$$\frac{1}{S} = \frac{1}{I_\lambda - \frac{1}{2}}. \quad (22)$$

We plot Eq. (22) in Figures 5 and 6. In these figures we have evaluated $\frac{1}{S}$ using Eq. (22) for 15 values of λ and interpolated for the other values of $\lambda \in [0, \frac{1}{2}]$. The calculations were carried out using a Riemann sum in which \mathcal{B}_∞ was divided into 4×10^5 squares. There is significant numerical artifact in Figure 6, as one really has $\frac{1}{S} \rightarrow 0$ as $\lambda \rightarrow \frac{1}{2}$ since $I_{\frac{1}{2}}$ diverges. For $\lambda < 0.3$ the curve Eq. (22) is approximately linear in λ . However, as λ approaches $\frac{1}{2}$ the slope become steeper, eventually approaching the vertical for $\lambda = \frac{1}{2}$. From this, we see that for sufficiently large spins S , the classical Néel state becomes a spin liquid at or near $\lambda = \frac{1}{2}$. For $\lambda > \frac{1}{2}$ the reduction is complex valued and thus has no physical significance. That this is so reflects the fact that the Néel state is not a ground

⁴There is however a typo in this result in [6]; that Eq. (21) is correct can be verified numerically using the plots contained in [6].

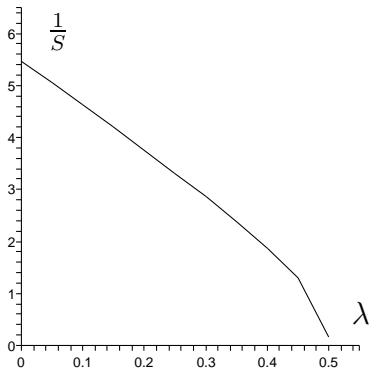


Figure 5: The phase diagram for the frustrated square lattice is plotted. The curve corresponds to the points at which the reduction Eq. (22) vanishes.

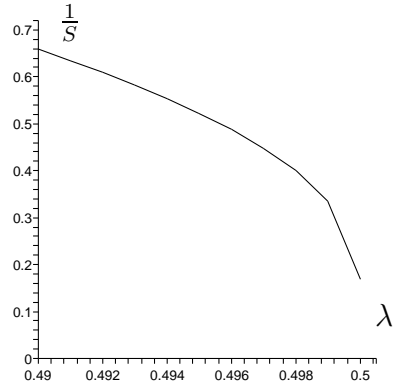


Figure 6: The phase diagram for the frustrated square lattice is plotted for λ close to $\frac{1}{2}$.

state for $\lambda > \frac{1}{2}$ due to the frustration and is thus not a suitable state to expand around for these values of λ . To understand the physics for $\lambda > \frac{1}{2}$ we must use spin wave analysis about a different state. See [6] for details and more analysis. We also see from Figure 5 that for arbitrary spin values S the Néel state is always melted at some $\lambda < \frac{1}{2}$.

6 Triangular Lattice

Having studied the Heisenberg model on the square lattice with nearest and next-nearest neighbour interactions, we now turn our attention to a second example. We would like to study the Heisenberg model on the triangular antiferromagnet with nearest and next-nearest neighbour interactions (Figure 7a). Recall that even with $J_2 = 0$ we saw that the triangular lattice is frustrated. Increasing $\lambda = \frac{J_2}{J_1}$ serves to increase this frustration, analogous to what we saw happen in the square lattice. The case $\lambda = 0$ was previously studied in [8]. The ground state in this case is the 120° state in which neighbouring spins are at 120° to each other (Figure 7b). This state naturally induces a three sublattice structure, the sublattices labeled by A , B and C , defined so that all spins on the same sublattice are collinear. Hence each primitive lattice cell contains exactly one vertex from each sublattice. Observe that $\vec{S}_a + \vec{S}_b + \vec{S}_c = 0$ if $a \in A$, $b \in B$ and $c \in C$ are all in the same primitive cell. We would like to dress the 120° state with spin waves for $\lambda \neq 0$ and thus generalizing the results in [8]. Since spins on the same sublattice are collinear it is clear that increasing λ increases frustration. We are motivated to consider this system as a function of λ because of the spin liquid structure discovered in the square lattice when $\lambda \neq 0$.

We approach this problem using two different methods, one using three types of Bosons and the other using only one type. As expected, the former is much more computationally intensive and for this reason we only set up the problem in this case. We also analyze the system from a classical

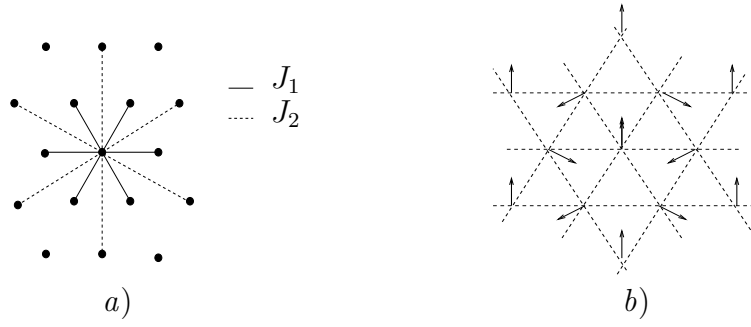


Figure 7: The figure shows i) the nearest and next-nearest neighbouring coupling in the frustrated triangular lattice, and ii) the 120° classical ground state.

perspective in the last subsection.

6.1 Three Boson Method

We use the three sublattices A , B and C constructed above for the 120° state. Denote the Bose operators on each sublattice by a_i , b_i and c_i , where i labels the point on the particular sublattice to which the operator is associated. Let $i, i' \in A$ be next-nearest neighbours. Using the Holstein-Primakoff transformation Eqs. (7), (8), (9) and the fact that \hat{S}_i and $\hat{S}_{i'}$ have a common quantization axis (their spins are collinear) we find

$$\hat{S}_i \cdot \hat{S}_{i'} = \left(\hat{S}_i^x \hat{S}_{i'}^x + \hat{S}_i^y \hat{S}_{i'}^y + \hat{S}_i^z \hat{S}_{i'}^z \right) = S^2 - S \left(a_i^\dagger a_i + a_{i'}^\dagger a_{i'} \right) + S \left(a_i^\dagger a_{i'} + a_i a_{i'}^\dagger \right)$$

Because spins on the A and B sublattices have different quantization axes the computation of the nearest neighbour interactions is slightly more involved. For example, if $j \in B$ is a nearest neighbour of i , we have

$$\begin{aligned} \hat{S}_i \cdot \hat{S}_j &= -S^2 + S \left(a_i^\dagger a_i + b_j^\dagger b_j \right) - \frac{S}{2} \left(a_i - a_i^\dagger \right) \left(b_j - b_j^\dagger \right) - \frac{S}{4} \left(a_i + a_i^\dagger \right) \left(b_j + b_j^\dagger \right) \\ &\quad + \frac{S}{2} \sqrt{\frac{3S}{2}} \left(\left(a_i - a_i^\dagger \right) - \left(b_j - b_j^\dagger \right) \right). \end{aligned}$$

Through cyclic permutations of a_i , b_i and c_i , all of the nearest neighbour terms are obtained. Combining the above results, the total Hamiltonian for the system can be written as

$$\begin{aligned} H &= (-J_1 + 3J_2) NS^2 + 3(J_1 - 2J_2) S \sum_{i,a} a_i^\dagger a_i + \frac{J_1 S}{4} \sum_{\langle i,j \rangle, a,b} \left(a_i b_j + a_i^\dagger b_j^\dagger \right) \\ &\quad - \frac{3J_1 S}{2} \sum_{\langle i,j \rangle, a,b} a_i^\dagger b_j + 2SJ_2 \sum_{\langle i,i' \rangle, a} a_i^\dagger a_{i'}. \end{aligned} \tag{23}$$

The notation $\sum_{\langle i,j \rangle, a,b}$ indicates first a sum over i and j , where i and j are nearest neighbours, followed by a sum over a_i and b_i , where $a_i, b_i \in \{a_i, b_i, c_i\}$. Note that Eq. (23) contains no linear

terms, as the cyclic permutation of a_i , b_i and c_i has canceled such terms. This is reassuring as classically we expect the 120° state to be a ground state, and hence stable. As linear terms in the Hamiltonian correspond to forces, we would therefore expect the Hamiltonian to have no such terms.

Next, we introduce the momentum space operators a_k , b_k and c_k , obtained from a_i , b_i and c_i via the Fourier transform. Because each sublattice is itself a triangular lattice, the Brillouin zone \mathcal{B} is a hexagon for each sublattice (see Appendix C). The calculations are algorithmic and yield

$$\begin{aligned} \frac{H}{6} = & (-1 + \lambda) J_1 N S^2 + J_1 S \sum_{k \in \mathcal{B}} [1 + \lambda(-1 + \beta_k)] \left(a_k^\dagger a_k + b_k^\dagger b_k + c_k^\dagger c_k \right) \\ & + \frac{J_1 S}{4} \sum_{k \in \mathcal{B}} \left[\alpha_k \left(a_k^\dagger b_k + b_k^\dagger c_k + c_k^\dagger a_k \right) + h.c. \right] - \frac{3J_1 S}{4} \sum_{k \in \mathcal{B}} \left[\alpha_k \left(a_k^\dagger b_{-k}^\dagger + b_k^\dagger c_{-k}^\dagger + c_k^\dagger a_{-k}^\dagger \right) + h.c. \right] \end{aligned} \quad (24)$$

where

$$\alpha_k = \frac{1}{3} \left(e^{-ik_x a} + 2e^{\frac{i}{2}k_x a} \cos \frac{\sqrt{3}}{2} k_z a \right) \quad (25)$$

and

$$\beta_k = \frac{1}{3} \left(\cos \sqrt{3} k_z a + 2 \cos \frac{3k_x a}{2} \cos \frac{\sqrt{3} k_z a}{2} \right). \quad (26)$$

The notation $h.c.$ indicates the hermitian conjugate of the preceding term. Note that $\alpha_k^* = \alpha_{-k}$ and $\beta_k^* = \beta_k$. For the special case of nearest neighbour interactions only, $\lambda = 0$, the Hamiltonian reduces to that obtained in [9]. We can also write Eq. (24) in matrix form. Define

$$\Delta = \begin{pmatrix} 0 & \alpha_k & \alpha_{-k} \\ \alpha_{-k} & 0 & \alpha_k \\ \alpha_k & \alpha_{-k} & 0 \end{pmatrix},$$

let I be the 3×3 identity matrix and let

$$\mathcal{H} = \begin{pmatrix} [1 + \lambda(-1 + \beta_k)] I + \frac{1}{4} \Delta & -\frac{3}{4} \Delta \\ -\frac{3}{4} \Delta & [1 + \lambda(-1 + \beta_k)] I + \frac{1}{4} \Delta \end{pmatrix}.$$

We can then write

$$\frac{H}{6} = (-1 + \lambda) J_1 N S^2 + \frac{J_1 S}{2} \sum_{k \in \mathcal{B}} \left[\left(a_k^\dagger \ a_{-k} \right) \mathcal{H} \begin{pmatrix} a_k \\ a_{-k}^\dagger \end{pmatrix} - 3 \right]. \quad (27)$$

We use the shorthand $\left(a_k^\dagger \ a_{-k} \right)$ for $\left(a_k^\dagger \ b_k^\dagger \ c_k^\dagger \ a_{-k} \ b_{-k} \ c_{-k} \right)$ and similarly for $\begin{pmatrix} a_k \\ a_{-k}^\dagger \end{pmatrix}$, which is just the conjugate transpose of $\left(a_k^\dagger \ a_{-k} \right)$. Following the usual diagonalization process we must

now find a Bogoliubov-Valatin transformation for the operators a_k , b_k and c_k , yielding a new set of Bose operators \mathbf{a}_k , \mathbf{b}_k and \mathbf{c}_k . In this case, the transformation can be written as a 6×6 matrix \mathcal{M} :

$$\begin{pmatrix} a_k \\ a_{-k}^\dagger \end{pmatrix} = \mathcal{M} \begin{pmatrix} \mathbf{a}_k \\ \mathbf{a}_{-k}^\dagger \end{pmatrix}.$$

Finding \mathcal{M} is non-trivial and computationally intensive. Because we can obtain our results by using an easier method, we do not attempt to construct \mathcal{M} . For a construction of \mathcal{M} in the special case $\lambda = 0$ see [13].

6.2 One Boson Method

As a second and simpler approach we use a single type of Bose operator to describe the spins in the triangular lattice. Then, for example, the Bose operator corresponding to a vertex on the A sublattice is a_1 and one on the B sublattice is a_2 , etc. We again perform calculations assuming each sublattice has N vertices and take the thermodynamic limit at the end of the calculation. Following a procedure analogous to that above, the Hamiltonian including only nearest neighbour interactions reads

$$\begin{aligned} H_{NN} = & -\frac{3}{2}J_1NS^2 + J_1S \sum \left(a_1^\dagger a_1 + a_2^\dagger a_2 + a_3^\dagger a_3 \right) - \frac{3}{4}J_1S \sum (a_1 a_2 + a_2 a_3 + a_3 a_1 + h.c.) \\ & + \frac{1}{4}S \sum \left(a_1 a_2^\dagger + a_2 a_3^\dagger + a_3 a_1^\dagger + h.c. \right) \end{aligned}$$

where the sums are over all combinations of nearest neighbours. We write the Bose operators in terms of the corresponding momentum space operators as

$$a_j = \frac{1}{\sqrt{N}} \sum_{k \in \mathcal{B}} e^{-ik \cdot r_j} a_k \quad \forall j \in \{1, 2, 3\}.$$

The first Brillouin zone \mathcal{B} is again hexagonal. We compute

$$\sum_{1,2} a_1 a_2 = \frac{1}{N} \sum_{1,2} \sum_{k \in \mathcal{B}} e^{-i(k+k') \cdot r_1} e^{-ik' \cdot \mathbf{r}_{12}} a_k a_{k'} = \sum_{k \in \mathcal{B}} \left(\sum_2 e^{-ik' \cdot \mathbf{r}_{12}} \right) a_k a_{-k}$$

where \mathbf{r}_{12} is a vector based at site $1 \in A$ and points to site $2 \in B$. Continuing we find that the Hamiltonian for nearest neighbour interactions written in terms of the momentum space operators is

$$H_{NN} = -\frac{3}{2}J_1NS^2 + 3J_1S \sum_{k \in \mathcal{B}} \left(1 + \frac{1}{2}\alpha_k \right) a_k^\dagger a_k - \frac{9}{4}J_1S \sum_{k \in \mathcal{B}} \alpha_k \left(a_k a_{-k} + a_k^\dagger a_{-k}^\dagger \right) \quad (28)$$

with

$$\alpha_k = \frac{1}{3} \left(\cos k_x a + 2 \cos \frac{1}{2} k_x a \cos \frac{\sqrt{3}}{2} k_z a \right). \quad (29)$$

These results agree with those obtained in [8]. By a similar calculation the Hamiltonian for the next-nearest neighbour interaction is found to be

$$H_{NNN} = 3J_2NS^2 - J_2S \sum_{i=1}^3 \sum_{\langle i,i' \rangle} \left(a_i^\dagger a_i + a_{i'}^\dagger a_{i'} \right) + J_2S \sum_{i=1}^3 \sum_{\langle i,i' \rangle} \left(a_i^\dagger a_{i'} + a_i a_{i'}^\dagger \right)$$

[This relation is correct. However, the passing to the old equation (30) is not; there is a factor of 2 missing in front of the λ in the non-constant term. We can see this as follows: both $a_i^\dagger a_i + a_{i'}^\dagger a_{i'}$ and $a_i^\dagger a_{i'} + a_i a_{i'}^\dagger$ are Fourier transformed to $2a_k^\dagger a_k$, where we use the commutation relation $[a_i, a_{i'}^\dagger] = \delta_{i,i'}$ to see that this holds for the second term. We then perform the sum $\sum_{i=1}^3$ to get the factor of $3 \times 2 = 6$, which is then summed over \mathcal{B} (this comes from the sum $\sum_{\langle i,i' \rangle}$; in the original calculation I neglected to take the factor of 2 into account.) After Fourier transforming, this is

$$H_{NNN} = 3J_2NS^2 + 6J_2S \sum_{k \in \mathcal{B}} (-1 + \beta_k) a_k^\dagger a_k \quad (30)$$

with

$$\beta_k = \frac{1}{3} \left(\cos \sqrt{3}k_z a + 2 \cos \frac{3k_x a}{2} \cos \frac{\sqrt{3}k_z a}{2} \right). \quad (31)$$

[The old equation (30) is

$$H_{NNN} = 3J_2NS^2 + 3J_2S \sum_{k \in \mathcal{B}} (-1 + \beta_k) a_k^\dagger a_k.$$

Note that there was no counting error in the constant term. This is also supported by the classical calculation performed in section 6.3. All of the equations below use the new result Eq. (33).]

Combining the above work, the total Hamiltonian is

$$H = \left(-\frac{3}{2} + 3\lambda \right) J_1NS^2 + 3J_1S \sum_{k \in \mathcal{B}} \left[\left(1 + \frac{1}{2}\alpha_k \right) + 2\lambda(-1 + \beta_k) \right] a_k^\dagger a_k - \frac{9}{4} J_1S \sum_{k \in \mathcal{B}} \alpha_k \left(a_k a_{-k} + a_k^\dagger a_{-k}^\dagger \right). \quad (32)$$

This is the same form as Eq. (12) which we know can be diagonalized by a Bogoliubov-Valatin transformation of the form Eq. (10). Enforcing the $c_k^\dagger c_{-k}^\dagger$ and $c_k c_{-k}$ terms vanish requires

$$\tanh 2\theta_k = \frac{\frac{3}{2}\alpha_k}{1 + \frac{1}{2}\alpha_k + 2\lambda(-1 + \beta_k)} \equiv \gamma_k.$$

Rewriting the Hamiltonian in terms of the Bogoliubov-Valatin transformation we find

$$H = H_\lambda^0 + \sum_{k \in \mathcal{B}} \omega_\lambda(k) \left(c_k^\dagger c_k + \frac{1}{2} \right)$$

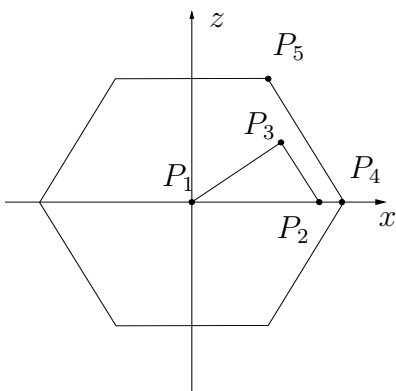


Figure 8: The path along the high symmetry lines of the Brillouin zone of the triangular lattice, where $P_1 = (0, 0)$, $P_2 = (\frac{4\pi}{3\sqrt{3}}, 0)$, $P_3 = (\frac{\pi}{\sqrt{3}}, \frac{2\pi}{3})$, $P_4 = (\frac{4\pi}{3}, 0)$ and $P_5 = (\frac{2\pi}{3}, \frac{2\pi}{\sqrt{3}})$.

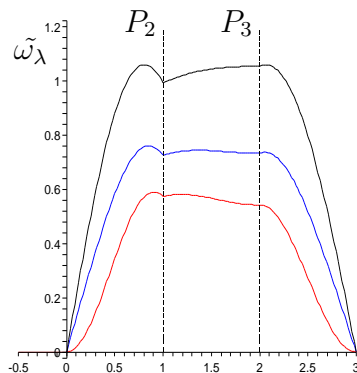


Figure 9: $\frac{\omega_\lambda(k)}{3J_1S} \equiv \tilde{\omega}_\lambda$, Eq. (33), is plotted for $\lambda = 0$ (black), $\lambda = 0.213$ (blue) and $\lambda = \frac{1}{3}$ (red) along the high symmetry curve $P_1P_2P_3$ of the Brillouin zone (see Figure 8). The points 0 and 3 on the horizontal axis correspond to P_1 .

with

$$\omega_\lambda(k) = 3J_1S \left[1 + \frac{1}{2}\alpha_k + 2\lambda(-1 + \beta_k) \right] \sqrt{1 - \gamma_k^2} \quad (33)$$

and

$$H_\lambda^0 = \left(-\frac{3}{2} + 3\lambda \right) NJ_1S^2.$$

[I have not corrected anything past here. Note however that figure 10 is still qualitatively the same, with the λ axis rescaled by a factor of 2, so that for instance, the slope goes to ∞ at $\lambda = \frac{1}{8}$ (at least numerically!) and the moment is completely reduced at $\lambda \approx 0.107$.]

We plot the spin wave frequencies $\frac{\omega_\lambda(k)}{3J_1S}$ in Figure 9 for three critical values of λ : $\lambda = 0$, in which case there are no next-nearest neighbour interactions, $\lambda = 0.213$ which will be seen below to be the value of λ that melts the 120° state, and $\lambda = \frac{1}{3}$, the largest value for which $\omega_\lambda(k)$ is real valued. The plot shows $\omega_\lambda(k)$ along the high symmetry path $P_1P_2P_3$ of the Brillouin zone (see Figure 8).

Using Eq. (20) we may now calculate the reduction of the moment due to the quantum fluctuations as a function of λ . We have

$$\frac{\langle \hat{S} \rangle}{S} = 1 - \frac{1}{2S} \frac{1}{A(\mathcal{B}_\infty)} \iint_{\mathcal{B}_\infty} d^2k \left(\frac{1 + \frac{1}{2}\alpha_k + \lambda(-1 + \beta_k)}{\sqrt{[1 + \frac{1}{2}\alpha_k + \lambda(-1 + \beta_k)]^2 - \frac{9}{4}\alpha_k^2}} - 1 \right) \quad (34)$$

where \mathcal{B}_∞ is the Brillouin zone in the thermodynamic limit and $A(\mathcal{B}_\infty)$ is its area. A straightforward calculation shows $A(\mathcal{B}_\infty) = \frac{8\pi^2}{\sqrt{3}}$. In the case of only nearest neighbour interactions, we find $\left. \frac{\langle \hat{S} \rangle}{S} \right|_{\lambda=0} \approx 1 - \frac{0.522}{2S}$ which agrees with the result obtained in [8]. Hence even for $\lambda = 0$ we see that the magnetic moment of the lattice is significantly reduced by the quantum fluctuations. We expect that as λ

grows the reduction will be even larger. Indeed, such behaviour is illustrated in Figure 10 where we plot Eq. (34) as a function of λ . This figure is obtained by calculating the reduction for 15 values of $\lambda \in [0, \frac{1}{4}]$ and interpolating. The integral Eq. (34) was approximated by a Riemann sum which divided \mathcal{B}_∞ into 3×10^5 squares. We find that for $\lambda \leq \frac{1}{4}$ the reduction is well defined while for $\lambda > \frac{1}{4}$ its value becomes complex. We will see below that this occurs because at $\lambda = \frac{1}{4}$ the 120° state becomes unstable, and thus cannot be used to expand around. For spin- $\frac{1}{2}$ particles, at approximately $\lambda = 0.213$ the state is completely melted, $\left. \frac{\langle \hat{S} \rangle}{S} \right|_{\lambda=0.213} \approx -0.001$. This estimate is found by dividing \mathcal{B}_∞ into 3×10^6 squares and using a Riemann sum. These results suggest that the $S = \frac{1}{2}$ frustrated triangular lattice may have a spin liquid ground state for $\lambda \approx 0.213$. We show now that this value of λ is very close the estimate provided by classical analysis.

6.3 Classical Results

We consider now the case of the classical ($S \rightarrow \infty$) Heisenberg model on a triangular antiferromagnet with nearest and next-nearest neighbour interactions to see if we can gain some understanding of the critical values of λ obtained above. We study two cases.

In the case that next-nearest neighbour interactions dominate, i.e. $J_2 \gg J_1$, we take as the ground state that with a decoupled 120° configuration on each of the three sublattices; we will call this the $3 - 120^\circ$ state. There are two degrees of freedom in its construction, the angle θ_{AB} between the A and B sublattices and the angle θ_{AC} between the A and C sublattices (see Figure 11). As such, the energy $E(\theta_{AB}, \theta_{AC})$ of the lattice is a function of the orientation of each sublattice. To calculate $E(\theta_{AB}, \theta_{AC})$ we first note that since the next-nearest neighbours of a given point lie on the same sublattice as that point, the energy of the lattice due to next-nearest neighbour interactions is independent of θ_{AB} and, θ_{AC} . We can write the energy due to nearest neighbour interactions

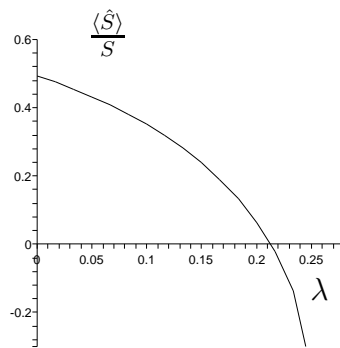


Figure 10: The reduction of the magnetic moment Eq. (34) is plotted using 15 sample points assuming $S = \frac{1}{2}$.

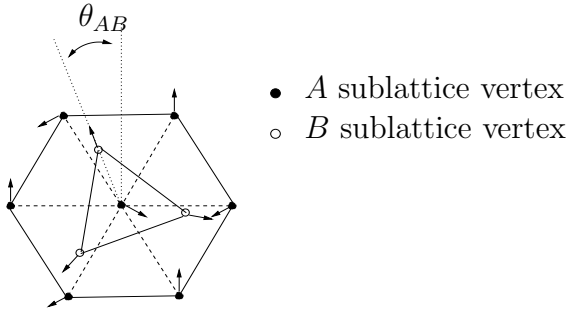


Figure 11: The relative orientations of the A and B sublattices.

between sublattices A and B as

$$E_{A,B}(\theta_{AB}) = \frac{1}{6} \sum_{\Delta_B} E_{A,\Delta_B}(\theta_{AB})$$

where Δ_B is a primitive triangle in the B sublattice, i.e. a triangle enclosing minimal area. We divide by 6 since each vertex is contained in 6 primitive lattice cells. Fixing Δ_B we find $E_{A,\Delta_B}(\theta_{AB}) = 3(\cos \theta_{AB} + \cos(\frac{2\pi}{3} - \theta_{AB}) + \cos(\frac{2\pi}{3} + \theta_{AB}))$. Recall that $\cos(x+y) + \cos(x-y) = 2\cos x \cos y$. Using this we find $E_{A,\Delta_B}(\theta_{AB}) \equiv 0$ which implies $E_{A,B}(\theta_{AB}) \equiv 0$. By symmetry, the energy of the nearest neighbour interactions for the entire lattice vanishes for all angles θ_{AB} and θ_{AC} . We find that the total energy of the lattice is then

$$\frac{E_{J_2 \gg J_1}(\theta_{AB}, \theta_{AC})}{J_1 N S^2} = -3\lambda. \quad (35)$$

Because the right hand side is independent of both θ_{AB} and θ_{AC} we see that classically for $J_2 \gg J_1$ the ground state of the frustrated triangular lattice is infinitely degenerate.

In the case that nearest neighbour interactions dominate, i.e. $J_1 \gg J_2$, the ground state of the lattice is the standard 120° state pictured in Figure 7b. A straightforward calculation shows that

$$\frac{E_{J_1 \gg J_2}}{J_1 N S^2} = -\frac{3}{2} + 3\lambda. \quad (36)$$

Note that this is the same as the constant term H_λ^0 in the diagonalized Hamiltonian obtained in Section 6.2, as it should be.

The critical value of λ at which Eqs. (35) and (36) give the same energy is $\lambda_0 = \frac{1}{4}$. We then see that for $\lambda < \lambda_0$, the 120° state has a lower energy, while for $\lambda > \lambda_0$, the $3 - 120^\circ$ structure has a lower energy. Hence, if the system begins in the 120° state and λ is increased at $\lambda = \lambda_0$ the $3 - 120^\circ$ state has lower energy, hence causing the 120° state to become unstable. Similarly, if the system is in the $3 - 120^\circ$ state then as λ passes below λ_0 the system becomes unstable. Thus λ_0 provides a rough estimate for what value of λ the frustrated triangular lattice may be melted and have a spin liquid ground state. From the spin wave analysis completed above we see that λ_0 is indeed an accurate estimate for where the onset of a spin liquid is likely to occur.

7 Discussion

We have successfully completed the first steps towards showing that the spin- $\frac{1}{2}$ Heisenberg antiferromagnet on the frustrated triangular lattice has spin liquid-like properties for sufficiently large $\lambda = \frac{J_2}{J_1}$. The critical value $\lambda_0 = \frac{1}{4}$ for which the classical 120° state becomes unstable and the system favours the $3 - 120^\circ$ state is the same value at which the reduction in the spin Eq. (34) becomes complex valued, reflecting the instability of the 120° state here. It was also found that the 120° state is melted for $\lambda \approx 0.213$, before it reaches its classical instability, which suggests that the system may have a quantum spin liquid ground state for sufficiently large λ in the region $(0.213, 0.25)$. Furthermore, for $\lambda > \lambda_0$ it was found that the $3 - 120^\circ$ state was infinitely degenerate which provides further support for the onset of an exotic state close to λ_0 .

It would be interesting to perform spin wave analysis on the $3 - 120^\circ$ state for an arbitrary choice of orientation angles θ_{AB} and θ_{AC} . The desired result would be to find the spin wave dispersion functions $\omega_{\lambda, \theta_{AB}, \theta_{AC}}(k)$ and compare the quantum zero-point energies $\frac{1}{2} \sum_k \hbar \omega_{\lambda, \theta_{AB}, \theta_{AC}}(k)$ as a function of θ_{AB} and θ_{AC} to see whether quantum fluctuations select a unique pair $(\tilde{\theta}_{AB}, \tilde{\theta}_{AC})$ yielding minimal energy for the system. We could then take $\lambda \rightarrow \lambda_0$ from the right to see whether the $3 - 120^\circ$ state also has characteristics of a spin liquid for sufficiently small λ . The computations involved in such calculations would be significantly more involved than those considered in the analysis for the 120° state, as the single boson method applied to each sublattice would still require three types of Bose operators, while the three boson method applied to each sublattice would require nine types of Bose operators, thus making the construction of a suitable Bogoliubov-Valatin transformation formidable. If a pair $(\tilde{\theta}_{AB}, \tilde{\theta}_{AC})$ were selected by quantum fluctuations, we would be able to study the state's symmetry groups to see which symmetries were broken in choosing the quantum ground state. There also remains the question as to whether the quantum ground state has some type of novel ordering unlike any of the orderings considered above. As finding novel orderings is of current interest it would be interesting to see whether or not the frustrated triangular lattice could provide a relatively simple example of this.

Also of interest is to understand the Heisenberg antiferromagnet on the frustrated tetrahedron, considered in Appendix D. It was shown that spin wave theory could not be used to analyze the quantum effects for $\lambda = 1$. Seeing how adding extra frustration, i.e. $\lambda \neq 0$, to the square and triangular lattices seemed to imply a spin liquid state for large enough λ leads one to conjecture that the same might occur in the single tetrahedron with frustration. Examining this case could then provide a simpler example of a three dimensional spin liquid than the pyrochlore lattice studied in [5], [19].

Appendix A: The Quantum Harmonic Oscillator

We briefly review the algebraic solution of the the quantum harmonic oscillator using Bose operators [12]. Under a suitable scaling of variables, the Hamiltonian describing the harmonic oscillator is

$$H = \frac{1}{2} (p^2 + x^2).$$

Define $a^\dagger = \frac{1}{\sqrt{2}}(x - ip)$ and $a = \frac{1}{\sqrt{2}}(x + ip)$. Then $[a, a^\dagger] = 1$. The Hamiltonian may be written in terms of a and a^\dagger as $H = a^\dagger a + \frac{1}{2}$. The spectrum of H is $\{n + \frac{1}{2} \mid n \in \{0\} \cup \mathbb{N}\}$ so that, in particular, the ground state of H has a non-vanishing energy $\frac{1}{2}$, or $\frac{1}{2}\hbar\omega$ where ω is the natural frequency of the oscillator.

Appendix B: Bloch's Theorem

The following theorem can be cast in many forms. In the context of sold state physics, it is usually referred to as Bloch's Theorem, discovered by Felix Bloch, while in the theory of differential equations it is most commonly known as Floquet's Theorem or the Floquet-Lyapunov Theorem, after Gaston Floquet and Alexander Lyapunov. For a proof in the context of quantum systems see [17].

Theorem 7.1 (Floquet (1883), Lyapunov (1892), Bloch (1928)). *Let $V(r)$ be a periodic potential with period $R \in (0, \infty)$, $V(r) = V(r + R) \quad \forall r \in \mathbb{R}$. Then the solutions of the Schrödinger equation*

$$-\frac{\hbar^2}{2m}\Delta\psi + V(r)\psi = E\psi$$

are of the form $\psi_k(r) = e^{ikr}\phi_k(r)$ and satisfy $\psi_k(r + R) = e^{ikR}\psi_k(r) \quad \forall r \in \mathbb{R}$.

Appendix C: The Brillouin Zone

Consider a two dimensional lattice whose primitive cell is determined by the vectors \vec{u}_1 and \vec{u}_2 . Define the two vectors \vec{v}_1 and \vec{v}_2 so that

$$\vec{u}_i \cdot \vec{v}_j = 2\pi\delta_{ij}.$$

Then \vec{v}_1 and \vec{v}_2 are primitive vectors of the reciprocal (momentum space) lattice. The primitive cell spanned by the vectors \vec{v}_1 and \vec{v}_2 is called the first Brillouin zone. The importance of the Brillouin zone stems from the fact that, by Bloch's Theorem, the solutions of the Schrödinger equation for a periodic lattice are characterized by their behavior in a single Brillouin zone.

We provide below an algorithm for determining the Brillouin zone given a two dimensional lattice. See [17] for details.

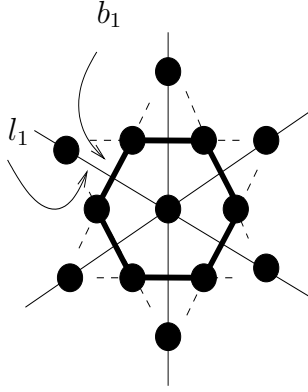


Figure 12: The first Brillouin zone of a triangular lattice is constructed.

- 1) Draw lines l_i between neighbouring vertices.
- 2) Draw the perpendicular bisector of each l_i ; call these b_i .
- 3) Fix a vertex. The region enclosed by the bisectors is the first Brillouin zone of the lattice.

To see how this process works, consider the triangular lattice, with primitive vectors $\vec{u}_1 = a\hat{x}$, $\vec{u}_2 = \frac{1}{2}a\hat{x} + \frac{\sqrt{3}}{2}a\hat{y}$. The process is illustrated in Figure 12. The resulting Brillouin zone \mathcal{B} is seen to be a hexagon in momentum space. Alternatively, we could use the first definition to find

$$\vec{v}_1 = \frac{\pi}{a} \left(2, -\frac{\sqrt{2}}{3} \right), \quad \vec{v}_2 = \frac{\pi}{a} \left(0, \frac{\sqrt{2}}{3} \right)$$

which would yield the same result.

Appendix D: The Heisenberg Model on a Single Tetrahedron

Both systems considered in the body of this work were two dimensional. As an extension, we consider the Heisenberg antiferromagnet on a single tetrahedron with nearest and next-nearest neighbour interactions, which is perhaps the simplest example of a fully frustrated three dimensional system. We simplify our calculations by noticing that we can view a tetrahedron as a linear chain with $N = 4$ vertices and periodic boundary conditions along with nearest and next-nearest neighbour interactions; such a lattice is homeomorphic to a single tetrahedron. This reduces the problem to one in a single dimension. Let J_1 and J_2 be the coupling constants for the nearest and next-nearest interactions, respectively. We proceed by expanding about the classical Néel state, in which neighbouring spins are anti-parallel. See Figure 13. Denote the vertices by A, B, C and D . Then, for nearest neighbours, say A and B , we have

$$\hat{S}_A \cdot \hat{S}_B = \left(\hat{S}_A^x \hat{x} + \hat{S}_A^y \hat{y} + \hat{S}_A^z \hat{z} \right) \cdot \left(\hat{S}_B^x \hat{x}' + \hat{S}_B^y \hat{y}' + \hat{S}_B^z \hat{z}' \right)$$

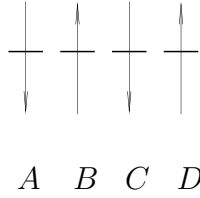


Figure 13: The Néel state on the $N = 4$ linear chain.

where the unprimed coordinate axis is that of A and the primed axis is that of B .⁵ We take the classical spins to be oriented along the z and z' axes. Denote by a^\dagger the Bose operator that creates a spin S on the A sublattice, with the analogous convention holding for the remaining vertices. Using the Holstein-Primakoff transformation Eqs. (7), (8) and (9) we have

$$\hat{S}_A \cdot \hat{S}_B = -S^2 + S(a^\dagger a + b^\dagger b) - S(ab + a^\dagger b^\dagger).$$

With analogous identities holding for the remaining nearest neighbour interactions, we find that the Hamiltonian including only nearest neighbour interactions is

$$H_{NN} = -4J_1 S^2 + 2J_1 S \sum_{j=1}^N a_j^\dagger a_j - J_1 S \sum_{j=1}^N (a_j a_{j+1} + a_j^\dagger a_{j+1}^\dagger) \quad (37)$$

where for notational simplicity we have set $a \mapsto a_1, \dots, d \mapsto a_4$. Similar calculations for next-nearest neighbours reveal

$$H_{NNN} = 2J_2 S^2 - J_2 S \sum_{j=1}^N a_j^\dagger a_j + J_2 S \sum_{j=1}^N a_j a_{j+2}^\dagger.$$

so that the full Hamiltonian is

$$H = (-4J_1 + 2\lambda) J_1 S^2 + (1 - \lambda) S \sum_{j=1}^N a_j^\dagger a_j - J_1 S \sum_{j=1}^N (a_j a_{j+1} + a_j^\dagger a_{j+1}^\dagger) + J_1 \lambda S \sum_{j=1}^N a_j a_{j+2}^\dagger \quad (38)$$

where $\lambda = \frac{J_2}{J_1}$. The Hamiltonian for the tetrahedron is recovered by setting $\lambda = 1$. Fourier transforming the Hamiltonian gives

$$H = (-4J_1 + 2J_2) S^2 + S \sum_{k \in \mathcal{B}} [2J_1 + J_2 (\cos 2k - 1)] a_k^\dagger a_k - J_1 S \sum_{k \in \mathcal{B}} \cos k (a_k a_{-k} + a_k^\dagger a_{-k}^\dagger).$$

The first Brillouin zone is $\mathcal{B} = \{-\frac{\pi}{2}, 0, \frac{\pi}{2}, \pi\}$. Although the Fourier transformed Hamiltonian is not diagonal, it is of the same form as Eq. (12), which we have shown to be diagonalizable using a Bogoliubov-Valatin transformation. Using the transformation Eq. (10), the requirement that the $c_k^\dagger c_{-k}^\dagger$ and $c_k c_{-k}$ terms vanish occurs if and only if

⁵Note that the hats on x, y, z denote the appropriate unit vectors of the coordinate system and not an operator.

$$\tanh 2\theta_k = \frac{\cos k}{1 + \lambda (\cos^2 k - 1)} \equiv \gamma_k. \quad (39)$$

In the case of only nearest neighbour interactions, $\lambda = 0$, this constraint on θ_k reduces that that derived in [16] for one dimension. For the full tetrahedron, $\lambda = 1$, we have $\gamma_k = \sec k \geq 1$. However, $\tanh 2\theta_k < 1$ for $\theta_k \in \mathbb{R}$, which suggests that the Bogoliubov transformation may not be valid for $\lambda = 1$, and perhaps other values of λ . We investigate this further below.

Rewriting the Hamiltonian using the Bogoliubov-Valatin transformation subject to the constraint Eq. (39) yields

$$H = H_\lambda^0 + \sum_{k \in \mathcal{B}} \omega_\lambda(k) \left(c_k^\dagger c_k + \frac{1}{2} \right) \quad (40)$$

where $\omega_\lambda(k) = 2J_1 S [1 + \lambda (\cos^2 k - 1)] \sqrt{1 - \gamma_k^2}$ and $H_\lambda^0 = (-4 + 2\lambda) J_1 (S^2 + S)$. With the above results we arrive at a formal expression for the ground state energy $E_\lambda^1 = H_\lambda^0 + \frac{1}{2} \sum_{k \in \mathcal{B}} \omega_\lambda(k)$ of the lattice including first order quantum fluctuations. For $\lambda \in [0, 1)$, we find

$$E_\lambda^1 = (-4 + 2\lambda) J_1 (S^2 + S) + 4J_1 S (1 - \lambda).$$

We exclude $\lambda = 1$ from the above result as there is a first order singularity in $\omega_{\lambda=1}(k)$ when $k = \pm \frac{\pi}{2}$ which prevents the formal sum $\sum_{k \in \mathcal{B}} \omega_\lambda(k)$ from being evaluated. Although the sum is well defined for $\lambda \in [0, 1)$ its validity here is uncertain as we claim that the Bogoliubov-Valatin transformation is not valid for $\lambda > \frac{1}{2}$. To see this, note that Eq. (39) implies that the requirement that $|\tanh 2\theta_k| < 1$ for all $\theta_k \in \mathbb{R}$ is equivalent to $\gamma_k^2 < 1$. This holds if and only if

$$0 < (1 - \lambda)^2 - (2\lambda^2 - 2\lambda + 1) \cos^2 k + \lambda^2 \cos^4 k$$

for all $k \in [-\pi, \pi]$. The right hand side has roots at $\cos^2 k = 1$ and $\cos^2 k = \left(\frac{\lambda-1}{\lambda}\right)^2$. The case $\cos^2 k = 1$ is independent of λ and is not the main cause of concern. Observe that for $\lambda > \frac{1}{2}$, $\left(\frac{\lambda-1}{\lambda}\right)^2 < 1$ so that the second root need be considered. That there exists $k_0 \in [-\pi, \pi]$ such that $\cos^2 k_0 = \left(\frac{\lambda-1}{\lambda}\right)^2$ is ensured by the Intermediate Value Theorem. From this we see that the Bogoliubov-Valatin transformation implemented is not well defined for $\lambda \in \left(\frac{1}{2}, 1\right]$, and hence Eq. (40) holds only for $\lambda \in \left[0, \frac{1}{2}\right)$.

One may wonder whether the choice $\mu_k = \cosh \theta_k$, $\eta_k = \sinh \theta_k$ is causing the problems. However, ones finds that for general μ_k and η_k subject to the normalization Eq. (11) the same problem occurs, so that it is indeed the Bogoliubov-Valatin transformation that is at fault.

The situation is even worse when we try to evaluate the the reduction of the moment using Eq. (20). Note that $\gamma_k = 1$ for $k \in \{0, \pi\}$ and $\lambda \in [0, 1)$, so that the reduction of the moment is not defined. It is suggested in [22] that to make sense of this the sum Eq. (20) should not be carried out over all of \mathcal{B} , but instead over $\mathcal{B} \setminus \{0, \pi\}$. Following this, we find that there is no reduction in the moment. In fact, [22] claims that in general the reduction of the moment will vanish in these

types of cases when considering finite lattices. Note however, that we can still say nothing about the case of the full tetrahedron, $\lambda = 1$.

Although we have not gained any physical understanding from the above calculations, we do understand why they did not work. We have seen that the Bogoliubov-Valatin transformation is not a valid method of diagonalizing the Hamiltonian, thus leaving spin wave theory insufficient to study the full tetrahedron. We must then use other techniques to study the quantum ground states of the frustrated single tetrahedron.

Acknowledgments

This thesis has been completed as part of PHYS 590 at Queen's University, Sept. 2006. through Apr. 2007. This work was graciously supervised by Dr. R. J. Gooding; the author is appreciative of his constant support and encouragement throughout the duration of the project.

References

- [1] Anderson, P. *Basic Notions of Condensed Matter Physics*. The Benjamin/Cummings Publishing Company, Menlo Park, Ca. 1984.
- [2] Anderson, P. Phys. Rev. **86** (5), 694 (1952).
- [3] Baskaran, G. Phys. Rev. Lett. **63** (22), 2524 (1989).
- [4] Binder, K. and Young, A. Rev. Mod. Phys. **58** (4), 801 (1986).
- [5] Canals, B. and Lacroix, C. Phys. Rev. Lett. **80** (13), 2933 (1998).
- [6] Chandra, P. and Doucot, B. Phys. Rev. B. **38** (13), 9335 (1988).
- [7] Cipra, B. Amer. Math. Monthly. **94** (10), 937 (1987).
- [8] Chubukov, A., Sachdev, S. and Senthil, T. J. Phys.: Condens. Matter. **6**, 8891 (1994).
- [9] Chubukov, A. and Golosov, D. J. Phys.: Condens. Matter. **3**, 69 (1991).
- [10] Feynman, R. *Statistical Mechanics: A Set of Lectures*. W. A. Benjamin, Inc. Reading, Mass. 1972.
- [11] Fukushima, H. et al. Prog. Theo. Phys. Supp. (145), 72 (2002).
- [12] Gustafson, S. and Sigal, I. *Mathematical Concepts of Quantum Mechanics*. Springer. New York, NY., 2003.

- [13] Jolicoeur, T. and Le Guillou, J. Phys. Rev. B. **40** (4), 2727 (1989).
- [14] Keffer, F., Kaplan, H. and Yafet, Y. Am. Jour. Phys. **21** (4), 250 (1953).
- [15] Kranendonk, J. and Van Vleck, J. Rev. Mod. Phys. **30** (1), 1 (1958).
- [16] Manousakis, E. Rev. Mod. Phys. **63** (1), 1 (1991).
- [17] Marder, M. *Condensed Matter Physics*. John Wiley & Sons, New York, N.Y. 2000.
- [18] Mila, F. Eur. J. Phys. **21**, 499 (2000).
- [19] Reimers, J., Berlinsky, A and Shi, A. Phys. Rev. B **34** (1), 865 (1991).
- [20] Towner, I. *PHYS 825 Course Notes*. Queen's University, Fall 2006.
- [21] van Vleck, J. Rev. Mod. Phys. **17** (1), 27 (1945).
- [22] Zhong, Q.F. and Sorella, S. Europhys. Lett. **21** (5), 629 (1993).